Taylor & Francis
Taylor & Francis Group

An electron electric dipole moment search in the $X^3\Delta_1$ ground state of tungsten carbide molecules

J. Lee[a], E.R. Meyer[b], R. Paudel[c], J.L. Bohn[b] and A.E. Leanhardt[a]*

[a]Department of Physics, University of Michigan, Ann Arbor, Michigan 48109-1040, USA;
[b]JILA, NIST and Department of Physics, University of Colorado, Boulder, Colorado 80309-0440, USA;
[c]Department of Physics, Wabash College, Crawfordsville, Indiana 47933-0352, USA

We identify the $X^3\Delta_1$ electronic ground state of tungsten carbide (WC) as a candidate molecular system in which to search for a permanent electric dipole moment (EDM) of the electron. The valence electrons in tungsten carbide experience an effective electric field of order $54\,\mathrm{GV\,cm^{-1}}$ when the molecule is placed in a laboratory electric field of just a few $\mathrm{mV\,cm^{-1}}$. Currently, a continuous tungsten carbide molecular beam is under construction. Tungsten atoms are evaporated from a resistively heated tungsten filament and are entrained in a noble gas jet containing a small fraction of methane. Tungsten carbide molecules are formed through the reaction $W + CH_4 \rightarrow WC + 2H_2$.

1. Introduction

The Standard Model of particle physics cannot explain several important experimental observations, for example why the strengths of the fundamental forces are so different (i.e. the hierarchy problem) and why there is a dominance of matter over anti-matter in the universe (i.e. baryogenesis). Various extensions to the Standard Model, most notably Supersymmetry (SUSY), have been developed with the goal of resolving these issues. These extensions predict 'new physics' that can be observed by experiments ranging in size from the Large Hadron Collider to laboratory-based tabletop precision measurements [1]. This work focuses on the latter, specifically, an electron electric dipole moment search using the valence electrons in the $X^3\Delta_1$ ground state of tungsten carbide molecules.

Any permanent electric dipole moment (EDM) violates both parity (P) and time-reversal (T) symmetries. According to the CPT Theorem, T-violation and CP-violation are equivalent such that EDMs enter the Standard Model through the CP-violating phase contained in the CKM Matrix [2]. For the electron, the Standard Model EDM prediction is limited to $|d_e| \approx 10^{-38}\,\mathrm{e\text{-}cm}$, while various extensions to the Standard Model predict electron EDMs that are over 10 orders of magnitude larger [3]. This gap between predictions provides a large window where a non-zero electron EDM signal would be a background-free discovery of physics beyond the Standard Model, while a null measurement would serve as a constraint for numerous theories. The discovery potential of EDM searches is not limited to the electron and experiments are underway in a variety of systems [4,5].

At present, the experimental limit on the electron EDM is $|d_e| < 1.6 \times 10^{-27}\,\mathrm{e\text{-}cm}$ [6]. To put a more intuitive size scale on this limit, we note $10^{-27}\,\mathrm{e\text{-}cm} \approx 5 \times 10^{-19}\,\mathrm{D}$, while typical induced (molecule-frame) electric dipole moments in polar molecules are of the order a few Debye. An electron EDM is manifest as an energy splitting between spin-up and spin-down states which is proportional to the effective electric field experienced by the electron.[1] This energy splitting, perhaps at the $h \times \mathcal{O}(\mathrm{mHz})$ level or below, must be resolved on top of residual Zeeman shifts that are typically several orders of magnitude larger. For example, the Stark shift of an electron EDM at the current experimental limit in one atomic unit of electric field is comparable to the Zeeman shift of a Bohr magneton in a magnetic field of only 1 nG.

The above comparison illuminates the need to apply enormous electric fields to the electron while maintaining exquisite control over residual Zeeman shifts. This can be accomplished by using the valence electrons in a suitably chosen heavy diatomic molecule [7]. To this end, the JILA EDM Group [8,9] has elucidated the benefits of heavy diatomic molecules in
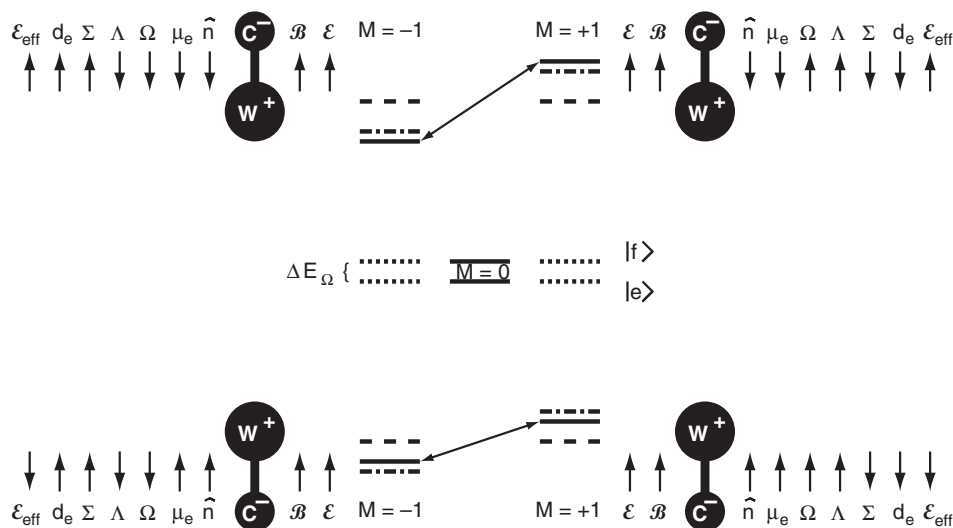
Figure 1. The $X^3\Delta_1$, $J=1$ ro-vibrational ground state of WC in external electromagnetic fields. In the absence of laboratory electric and magnetic fields, the ground state is split into a pair of $J=1$ parity eigenstates, $|e\rangle$ and $|f\rangle$, with a small energy separation ΔE_Ω (denoted as dotted lines for $|M|=1$ and solid lines for $M=0$). From here, applying a laboratory electric field, $\mathcal{E}$, mixes the states of opposite parity and shifts the $|M|=1$ states by an approximate energy $-\boldsymbol{\mu}_e \cdot \mathcal{E}$ to locations denoted by dashed lines. Next, in addition to the Stark shift, a laboratory magnetic field, $\mathcal{B}$, shifts the $|M|=1$ levels by an energy $gM\mu_B\mathcal{B}$ to locations denoted by dash-dot-dash lines. Finally, in addition to the Stark and Zeeman shifts, a non-zero electron electric dipole moment, d_e, shifts the $|M|=1$ levels by an energy $-\boldsymbol{d}_e \cdot \boldsymbol{E}_{eff}$ to their final locations denoted by solid lines. The difference in energy between the pair of $|\Delta M|=2$ transitions connected by arrows is $\sim 4d_e\mathcal{E}_{eff}$, which is nominally independent of the laboratory electric and magnetic fields. The energy splittings are not drawn to scale and $g>0$, $\mathcal{B}>0$, $d_e>0$ was assumed. The sign conventions are as follows: (i) the direction of the applied laboratory electric field, $\mathcal{E}$, defines the positive direction for the space-fixed quantization axis, (ii) the molecular axis, $\hat{n}$, is defined to point from carbon (C) to tungsten (W) and defines the positive direction for the molecule-fixed quantization axis, and (iii) the projection of the electronic spin along the molecular axis, Σ, defines the positive direction for the electron EDM, d_e. The projection of each vector quantity along the space-fixed quantization axis is indicated by $\uparrow$ or $\downarrow$ for the polarized molecular levels. See text for more details and definitions of various parameters.

$^3\Delta_1$ states for molecule-based electron EDM searches. In this work, we investigate the $X^3\Delta_1$ ground state of tungsten carbide (WC) [10], which adds to the work on metastable $^3\Delta_1$ states in HfF$^+$ [8,9,11], ThF$^+$ [8,12], and ThO [12–15].

2. Tungsten carbide molecular structure: an overview

Tungsten carbide has a $X^3\Delta_1$ ground state with its two valence electrons in a $\sigma\delta$ molecular orbital configuration [16–19].[2] The designation $^3\Delta_1$ is written as a term symbol, $^{2S+1}|\Lambda|_{|\Omega|}$, in the Hund's case (a) basis, which is not entirely accurate in the limit of large spin–orbit coupling, but will suffice for explanatory purposes. The two valence electrons in tungsten carbide form a $S=1$ spin triplet with projection $\Sigma = \mp 1$ along the molecular axis. Λ signifies a projection of the net electronic orbital angular momentum along the molecular axis of $\Lambda = \pm 2$. Finally, the projection of the total electronic angular momentum along the molecular axis is $\Omega = \Lambda + \Sigma = \pm 1$.

More generally, even in the limit of strong spin–orbit coupling, the ro-vibrational ground state of

tungsten carbide has total angular momentum $J=1$ with projections $M=0,\pm 1$ along a space-fixed quantization axis (Figure 1). Additionally, the $J=1$ ground state has a well-defined value of $|\Omega|=1$, which represents the projection of the *total* electronic angular momentum (spin *plus* orbital) along the molecular axis. In the absence of laboratory electric fields, the $J=1$ ground state is split into a pair of $J=1$ parity eigenstates, known as an Ω-doublet. For the $J=1$, $|\Omega|=1$ ground state of tungsten carbide, the Ω-doublet levels are labeled as $|e\rangle = |-\rangle = (|\eta; J, +|\Omega|, M\rangle - |\eta; J, -|\Omega|, M\rangle)/2^{1/2}$ and $|f\rangle = |+\rangle = (|\eta; J, +|\Omega|, M\rangle + |\eta; J, -|\Omega|, M\rangle)/2^{1/2}$, with odd ($-$) and even ($+$) parities, respectively, where η represents the any remaining labels necessary to fully specify the state.

The small energy splitting, $\Delta E_\Omega \sim h \times \mathcal{O}(\text{kHz})$, between Ω-doublet levels and relatively large induced electric dipole moment, $\mu_e \sim \mathcal{O}(\text{D})$, of the WC molecule, allows for a relatively weak laboratory electric field, $\mathcal{E} \sim \mathcal{O}(\text{mV cm}^{-1})$, to mix the states of opposite parity completely and to polarize the molecule fully. The dc laboratory electric field provides the space-fixed quantization axis for the remainder of the discussion. Furthermore, it only couples states with $\Delta M = 0$ and

an electric dipole selection rule forbids coupling between states with $\Delta J = 0$ and $\Delta M = 0$ for $M = 0$ levels. As such, the $M = 0$ levels do not mix and are nominally unaffected by laboratory electric and magnetic fields.[3] With a laboratory electric field applied, the energies of the $J = 1$, $|M| = 1$ levels follow $\pm[(\Delta E_\Omega / 2)^2 + (\mu_e \mathcal{E}/2)^2]^{1/2}$, where the zero of energy is taken at the midpoint of the Ω-doublet. In the limit $\mu_e \mathcal{E} \gg \Delta E_\Omega$, the $J = 1$, $|M| = 1$ levels are no longer eigenstates of parity and instead have (i) a definite value of the signed quantum number Ω and (ii) a non-zero effective electric field, $\mathcal{E}_{\text{eff}}$, experienced by the valence electrons, which is nominally *independent* of the applied laboratory electric field. A non-zero electron electric dipole moment, d_e, shifts the $|M| = 1$ levels by an energy $-\boldsymbol{d}_e \cdot \boldsymbol{\mathcal{E}}_{\text{eff}}$.

Several sources of systematic error are proportional to the laboratory electric field (e.g. Zeeman shifts due to (i) leakage currents and (ii) $\boldsymbol{v} \times \boldsymbol{\mathcal{E}}/c^2$ effective magnetic fields, where $\boldsymbol{v}$ is the velocity of molecules moving through the laboratory electric field $\boldsymbol{\mathcal{E}}$ and c is the speed of light), while a potential electron EDM signal is proportional to $\mathcal{E}_{\text{eff}}$. The saturation of $\mathcal{E}_{\text{eff}}$ when the molecule is fully polarized allows for a large variation of the laboratory electric field to search for systematic effects while leaving a true EDM signal unaffected. Furthermore, the small magnitude of $\mathcal{E}$ reduces the overall magnitude of these potential systematic errors, which is in sharp contrast to EDM searches using the valence electrons in atoms (Tl [6] and Cs [20–22]) and some molecules (YbF [23] and PbF [24]), where laboratory electric fields of order $10^5 \, \text{V cm}^{-1}$ and $10^4 \, \text{V cm}^{-1}$ must be applied, respectively.

For a laboratory magnetic field, $\boldsymbol{\mathcal{B}}$, applied parallel or anti-parallel to the electric field $\boldsymbol{\mathcal{E}}$, the $|M| = 1$ levels shift in energy by an amount $gM\mu_B \mathcal{B}$ due to the Zeeman effect, where g is the magnetic g-factor, μ_B is the Bohr magneton, and $\mathcal{B} > 0$ and $\mathcal{B} < 0$ represents $\boldsymbol{\mathcal{B}}$ parallel and anti-parallel to $\boldsymbol{\mathcal{E}}$, respectively. For a good Hund's case (a) state, the g-factor for a rotational level J is given by $g_J \approx \Omega(g_L \Lambda + g_S \Sigma)/J(J+1)$. For the $X^3\Delta_1$ ground state of tungsten carbide, $\Lambda = \pm 2$ and $\Sigma = \mp 1$, which yields $g_J \approx 0$ under the approximations $g_S \approx 2$ and $g_L \approx 1$ for the spin and orbital g-factors of the electron, respectively. Thus, the inherent sensitivity of the molecular levels to magnetic fields is significantly reduced compared to that of an unpaired valence electron in atoms such as Tl [6] and Cs [20–22] and molecules such as YbF [23] and PbO [25]. A similar reduction in the g-factor appears in the $^2\Pi_{1/2}$ state of PbF [24] and $^3\Delta_1$ states of HfF$^+$ [8,9,11], ThF$^+$ [8,12], and ThO [12–15]. Unfortunately, for the real $|\Omega| = 1$ states of WC, HfF$^+$, ThF$^+$, and ThO, the actual molecular g-factors will be dominated by admixtures of other Hund's case (a) electronic states with $|\Omega| = 1$ due

to strong spin–orbit coupling. The resultant g-factors are expected to be in the range $0.01 \lesssim g \lesssim 1$ and will be addressed further in the following section.

Even in the presence of a non-zero molecular g-factor, the pair of $|\Delta M| = 2$ transitions shown in Figure 1 share a common Zeeman shift. Thus, taking the difference between the transition energies yields a result, $4d_e \mathcal{E}_{\text{eff}}$, that is exclusively due to the electron EDM. This assumes that the g-factors of the upper and lower transitions are equal, which is a good approximation, but not an exact result [25]. The difference in g-factors and their dependence on the applied laboratory electric field will be addressed in the next section.

Above, we have provided a qualitative description of the $X^3\Delta_1$, $J = 1$ ro-vibrational ground state of tungsten carbide in the presence of laboratory electric and magnetic fields. In the next section, we will provide a non-relativistic molecular structure calculation to quantify these results.

3. Tungsten carbide molecular structure: a non-relativistic calculation

Our electronic structure calculation for tungsten carbide was similar to previous work on this molecule [16]. Specifically, we performed a non-relativistic multi-configuration, self-consistent field calculation [26] followed by a multi-reference configuration interaction calculation [27]. In order to assess the size of spin–orbit effects, additional scalar-relativistic calculations were performed. All calculations used the MOLPRO suite of codes [28]. For symmetry groups $\{A1, B1, B2, A2\}$, an active space of $\{9, 5, 5, 1\}$ orbitals were used, respectively, with $\{4, 2, 2, 0\}$ orbitals 'closed off' by constraining them to be doubly occupied. Closing off this space kept the calculation manageable and amounted to forcing orbitals that were bound by more than half an atomic unit of energy to be doubly occupied. The ECP60MWB scalar-relativistic potential of the Stuttgart group [29,30] was used to describe the 60 electron core as well as the s, p, d, f orbitals on tungsten and the aug-cc-pVTZ basis set of Dunning [31] was used to describe the s, p, d orbitals on carbon. Thus, the total number of electrons considered explicitly was 20.

The effective electric field calculation for tungsten carbide included the $X^3\Delta$ ground state and the $^5\Sigma^-$, $^3\Sigma^-$, $^5\Pi$, and $^1\Delta$ excited states, with relative energies similar to previous work [16]. A tungsten-to-carbon bond length of $r_0 = 1.727 \, \text{Å}$ was used for the $X^3\Delta$ ground state, which corresponds to the equilibrium bond length found previously [16]. This is longer than the experimental W–C bond length of $r_0 = 1.714 \, \text{Å}$ [17] due to relativistic contraction. Under these conditions, the calculated induced (molecule-frame) electric dipole

moment of WC is $\mu_e = 4.3\,D$, which is in good agreement with the value of $\mu_e = 4.2\,D$ calculated previously [16]. The polarization of tungsten carbide has the polarity W^+C^-, such that the induced (molecule-frame) electric dipole moment points *along* the molecular axis (i.e. from C^- to W^+). Using the perturbative approximation detailed in [12], the effective electric field experienced by the valence electrons in tungsten carbide is found to have magnitude $\mathcal{E}_{\mathrm{eff}} \approx 54\,\mathrm{GV\,cm^{-1}}$ and direction pointing *against* the molecular axis (i.e. from W^+ to C^-). We expect this estimate to be valid at the 25% level based on previous experience in comparing with more accurate calculations [12].

In addition to calculating $\mathcal{E}_{\mathrm{eff}}$, we also examined the magnitude of the Ω-doublet splitting, ΔE_Ω, and magnetic g-factor, g, in the $X^3\Delta_1$ ground state of WC. In a pure Hund's case (a) basis state, e.g. $^3\Delta_1$, the Ω-doublet splitting is more appropriately called Λ-type doubling and is caused by rotational and spin–orbit effects that mix in excited $^{2S+1}\Sigma_{|\Omega|}$ states of a particular parity. For WC in the $X^3\Delta_1$, $J=1$ ro-vibrational ground state, the negative parity state, $|e\rangle = |-\rangle$, is strongly influenced by relatively low-lying Σ^- states and therefore is lower in energy than the positive parity state, $|f\rangle = |+\rangle$, which is influenced by faraway Σ^+ states (Figure 1). The dominant contribution to the Λ-type doubling comes from couplings between the states $^3\Delta_1 \leftrightarrow {}^5\Pi_1 \leftrightarrow {}^5\Sigma_1^-$. The splitting can be computed with fourth-order perturbation theory by appropriately accounting for the many routes through which the perturbation can be transmitted [32]. In doing so, an order-of-magnitude estimate for the Ω-doublet splitting in the ro-vibrational ground state is $\Delta E_\Omega \approx h \times 1\,\mathrm{kHz}$, which is quite sensitive to the detailed energy differences between the intermediate electronic states. With an induced (molecule-frame) electric dipole moment of $\mu_e = 4.3\,D$, the electric field required to polarize WC is just a few $\mathrm{mV\,cm^{-1}}$.

The magnetic g-factor for the $X^3\Delta_1$ ground state is also affected by neighboring electronic states due to spin–orbit coupling. In particular, spin–orbit interactions mix a small amount of the $^5\Pi_1$ electronic state into the $X^3\Delta_1$ ground state. Using perturbation theory, the molecular g-factor can be estimated in terms of combinations of Hund's case (a) basis functions such that the leading-order contribution is $g_{J=1} \approx (1/2) \times ((E[^6D_{9/2}] - E[^6D_{1/2}])/4)/(E[^5\Pi_1] - E[^3\Delta_1]) \approx +0.12$, where $(E[^6D_{9/2}] - E[^9D_{1/2}])/4 \approx hc \times 1537\ \mathrm{cm^{-1}}$ [33] is the *average* ground state spin–orbit splitting for singly-ionized atomic tungsten[4] and $E[^5\Pi_1] - E[^3\Delta_1] \approx hc \times 6693\ \mathrm{cm^{-1}}$ [16]. Similar to the Ω-doublet splitting, this expression for the g-factor is a rough estimate and ultimately must be determined spectroscopically.

Without an applied laboratory electric field, the parity eigenstates, $|e\rangle$ and $|f\rangle$, have slightly different g-factors. These can be approximated as $g_{J=1}^f \approx g_{J=1} + 2(\Delta E_\Omega/hcB)$ and $g_{J=1}^e \approx g_{J=1} - 2(\Delta E_\Omega/hcB)$ [34], which yields a zero-field difference in g-factors potentially as small as $\Delta g(\mathcal{E}=0) \approx 4(\Delta E_\Omega/hcB) \approx 3 \times 10^{-7}$ for $\Delta E_\Omega/h \approx 1\,\mathrm{kHz}$ and $cB = 15\,\mathrm{GHz}$ [17]. Under the application of a laboratory electric field large enough to fully mix the parity eigenstates, the g-factors for the *upper* and *lower* transitions shown in Figure 1 deviate further. For $^3\Delta_1$ molecules in the ground rotational state, the leading order correction to $g_{J=1}$ is due to an interference between the Stark mixing and Zeeman mixing of the $J=2$ rotational excited state. The difference in g-factors scales as $\Delta g(\mathcal{E})/g_{J=1} = (g_{\mathrm{upper}} - g_{\mathrm{lower}})/g_{J=1} \approx +(3/10)(\mu_e\mathcal{E}/hcB)$ [25]. In the limit $\mu_e\mathcal{E} \gg \Delta E_\Omega$, the electric field dependent g-factor difference will be comparable to, if not larger than, the zero field g-factor difference. For WC molecules in a laboratory electric field of $\mathcal{E} \approx 1\,\mathrm{V\,cm^{-1}}$, the absolute difference between g-factors for the *upper* and *lower* transitions shown in Figure 1 is estimated to be $\Delta g(\mathcal{E} \approx 1\,\mathrm{V\,cm^{-1}}) \approx 5 \times 10^{-6}$ for $g_{J=1} \approx +0.12$, $\mu_e \approx 4.3\,D$, and $cB = 15\,\mathrm{GHz}$ [17]. As a result, the energy difference between a pair of $|\Delta M| = 2$ transitions shown in Figure 1 will have a small laboratory electric field and magnetic field dependence, rather than simply being equal to $4d_e\mathcal{E}_{\mathrm{eff}}$.

4. Continuous tungsten carbide molecular beam

As a precursor to creating a continuous tungsten carbide molecular beam, we have first developed a continuous tungsten atomic beam. Tungsten atoms are continuously evaporated from a resistively heated filament by passing a dc current through it. For a filament diameter $\sim 500\,\mu\mathrm{m}$, a current of $\sim 25\,\mathrm{A}$ heats the filament to a temperature of $\sim 3000\,\mathrm{K}$. Typically, (i) the total number of tungsten atoms evaporated from a single filament before it breaks is $\sim 10^{19}$, as measured by the change in diameter of the filament, and (ii) the filament lifetime is $\sim 1000\,\mathrm{s}$, but can be made arbitrarily shorter or longer by varying the current by a few amps.

The filament is surrounded by ~ 1 torr of argon buffer gas. The majority of tungsten atoms evaporated from the filament are entrained in a buffer gas jet that forms by passing through a converging–diverging conical nozzle (half-angle $\sim 15°$) upon entering a high vacuum region. The measured beam divergence after exiting the nozzle is $\sim 50\,\mathrm{mrad}$. The beam propagates $\sim 30\,\mathrm{cm}$ before passing through a 3 mm diameter copper skimmer, after which the measured beam divergence is only $\sim 5\,\mathrm{mrad}$. This results in a factor of ~ 100 reduction in the atomic flux. A glass slide placed
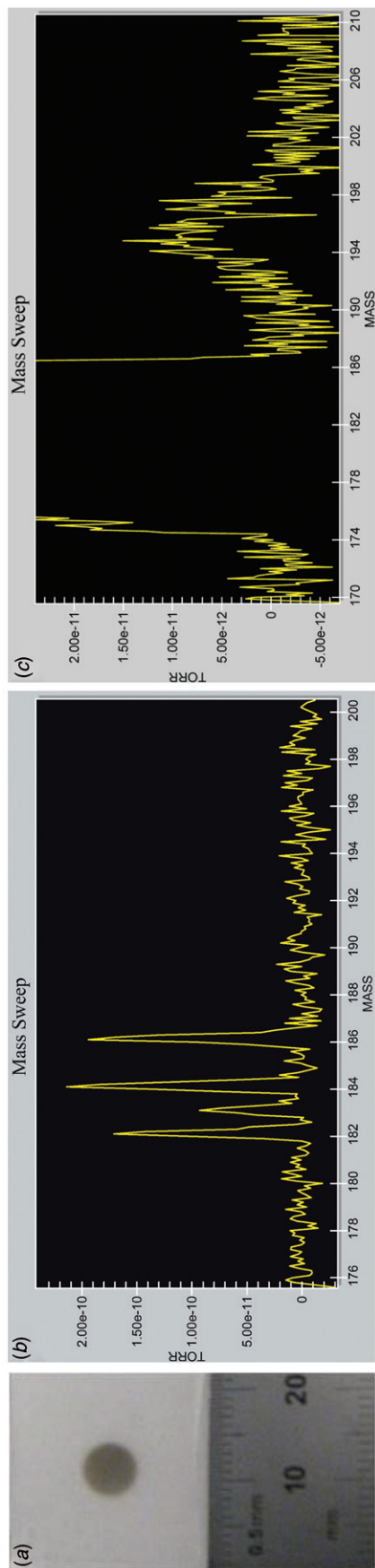
Figure 2. (*a*) Tungsten atoms sputtered onto a glass slide placed ~30 cm downstream from a 3 mm diameter skimmer. (*b*), (*c*) Quadrupole mass spectra of tungsten atoms (masses 182, 183, 184, and 186 amu) evaporated from a resistively heated tungsten filament in vacuum and tungsten carbide molecules (masses 194, 195, 196, and 198 amu) formed by resistively heating a tungsten filament in the presence of an argon + methane buffer gas. (The color version of this figure is included in the online version of the journal.)

~30 cm after the skimmer collects the tungsten atoms for analysis (Figure 2(*a*)). The deposited tungsten spot has a diameter of ~6 mm and a thickness of ~30 nm, corresponding to ~5×10^{16} tungsten atoms and a flux of ~10^{21} tungsten atoms per steradian per filament. Converting the continuous tungsten atomic beam to a continuous tungsten carbide molecular beam can be accomplished by adding a small fraction of methane to the buffer gas. This allows for the chemical reaction $W + CH_4 \rightarrow WC + 2H_2$, which we have observed using a quadrupole mass filter (Figures 2(*b*) and (*c*)).

Optical spectroscopy of the WC molecules is currently under development to determine the flux and ro-vibrational state occupation of the WC molecules. Additionally, tungsten carbide has abundant isotopes $^{182}W^{12}C$ (26%), $^{184}W^{12}C$ (30%), and $^{186}W^{12}C$ (28%) with zero nuclear spin and thus no hyperfine structure, which will greatly simplify the electron EDM measurement, while $^{183}W^{12}C$ (14%) has hyperfine structure due to a tungsten nuclear spin of $I = 1/2$. Comparing a measurement of the hyperfine structure in $^{183}W^{12}C$ to theoretical calculations will be useful in characterizing the electronic wavefunction overlap with the tungsten nucleus, which can potentially improve calculations and uncertainty estimates of $\mathcal{E}_{\text{eff}}$. Future measurements probing nuclear Schiff moments [5] may also be possible in $^{183}W^{12}C$.

5. EDM sensitivity considerations

Given the effective electric field experienced by the valence electrons in the polarized $X^3\Delta_1$ ground state of tungsten carbide, $\mathcal{E}_{\text{eff}} \approx 54\,\text{GV cm}^{-1}$, an electron EDM just below the current experimental limit, $|d_e| < 1.6 \times 10^{-27}$ e-cm [6], would produce a frequency shift to the spectroscopy transitions shown in Figure 1 of $\Delta\omega_{\text{EDM}} = 2d_e\mathcal{E}_{\text{eff}}/\hbar \approx 2\pi \times 40\,\text{mHz}$. Given round, but reasonable, parameters for typical molecular beams, such as a mean beam speed of $v \approx 1000\,\text{m s}^{-1}$ and a length of $L \approx 1\,\text{m}$ corresponding to an interrogation time of $\tau \approx 1\,\text{ms}$, the Fourier-limited frequency resolution of a single-particle measurement is $\delta\omega_{\text{stat}} = 1/\tau \approx 2\pi \times 160\,\text{Hz}$. Thus, to achieve a statistical sensitivity for detecting an electron EDM just below the current limit, we would require of order $N \approx 16 \times 10^6$ WC molecules to be interrogated. Improving upon the current electron EDM limit by a factor of ~1000 would require of order $N \approx 16 \times 10^{12}$ WC molecules to be interrogated, corresponding to statistical frequency resolution of $\delta\omega_{\text{stat}}/N^{1/2} \approx 2\pi \times 40\,\mu\text{Hz}$.

Major systematic concerns arise from spurious Zeeman shifts. Most of these can be removed by taking the difference in frequencies between the *upper* and *lower* transitions shown in Figure 1, provided that the g-factors for the separate transitions are identical and/or well known. Assuming that an upper bound on the *uncertainty* in g-factors, δg can be approximated through the g-factor difference estimated above, $\delta g \approx \Delta g(\mathcal{E} \approx 1\,\text{V cm}^{-1})/2 \approx 2.5 \times 10^{-6}$, then this sets an upper bound on our ability to differentiate Zeeman shifts from true EDM signals and gives rise to a systematic limit for the experiment: $\delta\omega_{\text{sys}} \approx 2(\delta g)M\mu_B \mathcal{B}/\hbar$. Under this assumption, a residual magnetic field of $\mathcal{B} \approx 6\,\text{mG}$ would give rise to a systematic uncertainty in the transition frequencies, $\delta\omega_{\text{sys}} \approx 2\pi \times 40\,\text{mHz}$, limiting the sensitivity to the experiment to detecting an electron EDM near the current limit. Correspondingly, magnetic field control at the $\mathcal{B} \approx 6\,\mu\text{G}$ level would reduce the potential systematic uncertainty to a factor of ~1000 below the current electron EDM limit.

6. Conclusion

Molecular states with the $^3\Delta_1$ symmetry are good candidates for electron EDM searches because their valence electrons experience a large effective electric field under the application of only a weak laboratory electric field and have a small magnetic moment. Additionally, $^3\Delta_1$ states have a pair of spectroscopy transitions with similar sensitivities to magnetic fields, but sensitivities to an electron EDM with opposite signs, such that they have a built-in co-magnetometer to monitor for spurious Zeeman shifts. To our knowledge, tungsten carbide is the only heavy diatomic molecule verified both theoretically [16,18] and experimentally [17,19] to have a $^3\Delta_1$ ground state. However, $^3\Delta_1$ molecular levels arise as a low-lying metastable state in other species currently being used for electron EDM searches (e.g. HfF$^+$ [8,9], ThF$^+$ [8,12], and ThO [12–15]). For WC, we have calculated $\mathcal{E}_{\text{eff}} \approx 54\,\text{GV cm}^{-1}$ under the application of a laboratory field of just a few mV cm^{-1}. Furthermore, the magnetic g-factor of the ro-vibrational ground state was estimated to be $g \approx +0.12$ with g-factor differences between the fully polarized Ω-doublet levels estimated to be at the level of $\Delta g(\mathcal{E} \approx 1\,\text{V cm}^{-1}) < \mathcal{O}(10^{-5})$. A continuous tungsten atomic beam has been developed with a flux of ~10^{21} tungsten atoms per steradian per filament, and we are currently working towards converting this to a continuous tungsten carbide molecular beam.

Notes

1. There are solid state electron EDM searches that look for an induced magnetic field under an applied voltage [35] or an induced voltage under an applied magnetic field [36].

2. To our knowledge, there is one published calculation that disagrees with the $^3\Delta_1$ assignment for the ground state of tungsten carbide [37].

3. All M levels of the $J = 1$ rotational ground state will mix with the corresponding M levels of the $J = 2$ rotationally excited state, however, this mixing will be minimal for sufficiently weak laboratory electric fields in the limit $\Delta E_\Omega \ll \mu_e \mathcal{E} \ll hcB$, where h is the Planck constant, c is the speed of light, and B is the rotational constant of the molecular state.

4. The *average* energy splitting for the singly-ionized atomic tungsten electronic ground state, $(E[^6D_{9/2}] - E[^6D_{1/2}])/4 \approx hc \times 1537\,\text{cm}^{-1}$, was taken to be the relevant spin–orbit splitting since the tungsten carbide bond is fairly ionic, i.e. W^+–C^-. Using the *average* energy splitting for the neutral atomic tungsten electronic ground state, $(E[^5D_4] - E[^5D_0])/4 \approx hc \times 1555\,\text{cm}^{-1}$ does not significantly modify the calculation.

References

[1] Jung, S.; Wells, J.D. Comparison of Electric Dipole Moments and the Large Hadron Collider for Probing CP Violation in Triple Boson Vertices. 2008, arXiv:0811.4140v1 e-Print archive. http://arxiv.org/abs/0811.4140.

[2] Amsler, C.; Doser, M.; Antonelli, M.; Asner, D.M.; Babu, K.S.; Baer, H.; Band, H.R.; Barnett, R.M.; Bergren, E.; Beringer, J.; Bernardi, G.; Bertl, W.; Bichsel, H.; Biebel, O.; Bloch, P.; Blucher, E.; Blusk, S.; Cahn, R.N.; Carena, M.; Caso, C.; Ceccucci, A.; Chakraborty, D.; Chen, M.-C.; Chivukula, R.S.; Cowan, G.; Dahl, O.; D'Ambrosio, G.; Damour, T.; de Gouvêa, A.; DeGrand, T.; Dobrescu, B.; Drees, M.; Edwards, D.A.; Eidelman, S.; Elvira, V.D.; Erler, J.; Ezhela, V.V.; Feng, J.L.; Fetscher, W.; Fields, B.D.; Foster, B.; Gaisser, T.K.; Garren, L.; Gerber, H.-J.; Gerbier, G.; Gherghetta, T.; Giudice, G.F.; Goodman, M.; Grab, C.; Gritsan, A.V.; Grivaz, J.-F.; Groom, D.E.; Grünewald, M.; Gurtu, A.; Gutsche, T.; Haber, H.E.; Hagiwara, K.; Hagmann, C.; Hayes, K.G.; Hernández-Rey, J.J.; Hikasa, K.; Hinchliffe, I.; Höcker, A.; Huston, J.; Igo-Kemenes, P.; Jackson, J.D.; Johnson, K.F.; Junk, T.; Karlen, D.; Kayser, B.; Kirkby, D.; Klein, S.R.; Knowles, I.G.; Kolda, C.; Kowalewski, R.V.; Kreitz, P.; Krusche, B.; Kuyanov, Yu.V.; Kwon, Y.; Lahav, O.; Langacker, P.; Liddle, A.; Ligeti, Z.; Lin, C.-J.; Liss, T.M.; Littenberg, L.; Liu, J.C.; Lugovsky, K.S.; Lugovsky, S.B.; Mahlke, H.; Mangano, M.L.; Mannel, T.; Manohar, A.V.; Marciano, W.J.; Martin, A.D.; Masoni, A.; Milstead, D.; Miquel, R.; Mönig, K.; Murayama, H.; Nakamura, K.; Narain, M.; Nason, P.; Navas, S.; Nevski, P.; Nir, Y.; Olive, K.A.; Pape, L.; Patrignani, C.; Peacock, J.A.; Piepke, A.; Punzi, G.; Quadt, A.; Raby, S.; Raffelt, G.; Ratcliff, B.N.; Renk, B.; Richardson, P.; Roesler, S.; Rolli, S.; Romaniouk, A.; Rosenberg, L.J.; Rosner, J.L.; Sachrajda, C.T.; Sakai, Y.; Sarkar, S.; Sauli, F.; Schneider, O.; Scott, D.; Seligman, W.G.; Shaevitz, M.H.; Sjöstrand, T.; Smith, J.G.; Smoot, G.F.; Spanier, S.; Spieler, H.; Stahl, A.; Stanev, T.; Stone, S.L.; Sumiyoshi, T.; Tanabashi, M.; Terning, J.; Titov, M.; Tkachenko, N.P.; Törnqvist, N.A.; Tovey, D.; Trilling, G.H.; Trippe, T.G.; Valencia, G.; van Bibber, K.; Vincter, M.G.; Vogel, P.; Ward, D.R.; Watari, T.; Webber, B.R.; Weiglein, G.; Wells, J.D.; Whalley, M.; Wheeler, A.; Wohl, C.G.; Wolfenstein, L.; Womersley, J.; Woody, C.L.; Workman, R.L.; Yamamoto, A.; Yao, W.-M.; Zenin, O.V.; Zhang, J.R.-Y.; Zyla, P.A. *Phys. Lett. B* **2008,** *667,* 1–1340.

[3] Pospelov, M.; Ritz, A. *Ann. Phys.* **2005,** *318,* 119–169.

[4] Commins, E.D. *J. Phys. Soc. Jpn.* **2007,** *76,* 111010.

[5] Griffith, W.C.; Swallows, M.D.; Loftus, T.H.; Romalis, M.V.; Heckel, B.R.; Fortson, E.N. *Phys. Rev. Lett.* **2009,** *102,* 101601.

[6] Regan, B.C.; Commins, E.D.; Schmidt, C.J.; DeMille, D. *Phys. Rev. Lett.* **2002,** *88,* 071805.

[7] Hinds, E.A. *Physica Scripta* **1997,** *T70,* 34–41.

[8] Cornell Group. http://jilawww.colorado.edu/bec/CornellGroup/

[9] Meyer, E.R.; Bohn, J.L.; Deskevich, M.P. *Phys. Rev. A* **2006,** *73,* 062108.

[10] Lee, J.; Paudel, R.; Leanhardt, A.E. Presented at ICAP XXI, University of Connecticut, CT, USA, July 27–August 1, 2008; Poster TU1.

[11] Petrov, A.N.; Mosyagin, N.S.; Titov, A.V. *Phys. Rev. A* **2009,** *79,* 012505.

[12] Meyer, E.R.; Bohn, J.L. *Phys. Rev. A* **2008,** *78,* 010502.

[13] Meyer, E.; Bohn, J. *Bull. Am. Phys. Soc.* **2008,** *53,* 28.

[14] Vutha, A.C.; Baker, O.K.; Campbell, W.C.; DeMille, D.; Doyle, J.M.; Gabrielse, G.; Gurevich, Y.V.; Jansen, M.A.H.M. *Bull. Am. Phys. Soc.* **2008,** *53,* 28.

[15] Vutha, A.C.; Baker, O.K.; Campbell, W.C.; Doyle, J.M.; Gabrielse, G.; Gurevich, Y.V.; Hamilton, P.; Hutzler, N.; Jansen, M.A.H.M.; DeMille, D. Presented at ICAP XXI, University of Connecticut, CT, USA, July 27–August 1, 2008; Poster TU2.

[16] Balasubramanian, K. *J. Chem. Phys.* **2000,** *112,* 7425–7436.

[17] Sickafoose, S.M.; Smith, A.W.; Morse, M.D. *J. Chem. Phys.* **2002,** *116,* 993–1002.

[18] Stevens, F.; Carmichael, I.; Callens, F.; Waroquier, M. *J. Phys. Chem. A* **2006,** *110,* 4846–4853.

[19] Rothgeb, D.; Hossain, E.; Jarrold, C.C. *J. Chem. Phys.* **2008,** *129,* 114304.

[20] Heinzen, D.J. http://www.ph.utexas.edu/~coldatom/

[21] Amini, J.M.; Munger Jr, C.T.; Gould, H. *Phys. Rev. A* **2007,** *75,* 063416.

[22] Fang, F.; Weiss, D.S. *Opt. Lett.* **2009,** *34,* 169–171.

[23] Hudson, J.J.; Sauer, B.E.; Tarbutt, M.R.; Hinds, E.A. *Phys. Rev. Lett.* **2002,** *89,* 023003.

[24] Shafer-Ray, N.E. *Phys. Rev. A* **2006,** *73,* 034102.

[25] Bickman S.; Hamilton, P.; Jiang, Y.; DeMille, D. Preparation and Detection of States with Simultaneous Spin Alignment and Molecular Orientation in PbO. 2008, arXiv:0807.4851v1. e-Print archive. http://arxiv.org/abs/0807.4851.

[26] Werner, H.J.; Knowles, P.J. *J. Chem. Phys.* **1985,** *82,* 5053–5063.

[27] Knowles, P.J.; Werner, H.J. *Chem. Phys. Lett.* **1985,** *115,* 259–267.

[28] Werner, H.-J.; Knowles, P.J.; Lindh, R.; Manby, F.R.; Schütz, M.; Celani, P.; Korona,T.; Mitrushenkov, A.; Rauhut, G.; Adler, T.B.; Amos, R.D.; Bernhardsson, A.; Berning, A.; Cooper, D.L.; Deegan, M.J.O.; Dobbyn, A.J.; Eckert, F.; Goll, E.; Hampel, C.; Hetzer, G.; Hrenar, T.; Knizia, G.; Köppl, C.; Liu, Y.; Lloyd, A.W.; Mata, R.A.; May, A.J.; McNicholas, S.J.; Meyer, W.; Mura, M.E.; Nicklaß, A.; Palmieri, P.; Pflüger, K.; Pitzer, R.; Reiher, M.; Schumann, U.; Stoll, H.; Stone, A.J.; Tarroni, R.; Thorsteinsson, T.; Wang, M.; Wolf, A. MOLPRO, version 2008.1. http://www.molpro.net/.

[29] Andrae, D.; Häussermann, U.; Dolg, M.; Stoll, H.; Preuß, H. *Theor. Chim. Acta* **1990,** *77,* 123–141.

[30] Martin, J.; Sundermann, A. *J. Chem. Phys.* **2001,** *114,* 3408–3420.

[31] Dunning Jr, T.H. *J. Chem. Phys.* **1989,** *90,* 1007–1023.

[32] Brown, J.M.; Cheung, A.S.C.; Merer, A.J. *J. Mol. Spect.* **1987,** *124,* 464–475.

[33] Sansonetti, J.E.; Martin, W.C.; Young, S.L. Handbook of atomic spectroscopic data. http://physics.nist.gov/PhysRefData/Handbook/

[34] Nelis, T.; Beaton, S.P.; Evenson, K.M.; Brown, J.M. *J. Mol. Spect.* **1991,** *148,* 462–478.

[35] Liu, C.Y.; Lamoreaux, S.K. *Mod. Phys. Lett. A* **2004,** *19,* 1235–1238.

[36] Heidenreich, B.J.; Elliott, O.T.; Charney, N.D.; Virgien, K.A.; Bridges, A.W.; McKeon, M.A.; Peck, S.K.; Krause Jr, D.; Gordon, J.E.; Hunter, L.R.; Lamoreaux, S.K. *Phys. Rev. Lett.* **2005,** *95,* 253004.

[37] Wang, J.; Sun, X.; Wu, Z. *J. Clust. Sci.* **2007,** *18,* 333–344.